Desalination and Water Treatment
www.deswater.com
doi:10.5004/dwt.2021.27143

225 (2021) 413–421
June

Effect of ultrasound on biosorption kinetics of Acid blue 25 from aqueous media by using cycads palm bark as novel biosorbent

Sana Haou[a], El Khamssa Guechi[a,*], Soulef Benabdesselam[b], Oualid Hamdaoui[a]

[a]*Laboratory of Environmental Engineering, Department of Process Engineering, Faculty of Engineering, Badji Mokhtar – Annaba University, P.O. Box: 12, 23000 Annaba, Algeria, email: guichi_wahida@yahoo.fr*
[b]*Laboratory of Environmental and Water Engineering in Saharan Environment, Department of Process Engineering, Faculty of Applied Sciences, Kasdi Merbah-Ouargla University, Ouargla, Algeria*

Received 3 February 2020; Accepted 29 January 2021

ABSTRACT

In this work, the cycads palm bark (CPB) was tested as a novel biosorbent for the removal of acid blue 25 (AB25) from aqueous media in the absence and presence of ultrasonic irradiation. Batch biosorption studies were conducted to study the effects of different parameters such as initial pH solution, biosorbent dose, initial dye concentration, and ultrasonic power on AB25 dye biosorption in order to explain the influence of ultrasonic irradiation on biosorption kinetics. Ultrasonic irradiation and initial pH solution played a key role in the removal of acid dye. The amount of AB25 biosorption is markedly increased in the presence of the ultrasonic field and reduces of equilibrium time for biosorption. The biosorption kinetic data were found to be well-represented by the pseudo-second-order rate equation, both in the absence and presence of ultrasound. The activation energy (E_a) of biosorption has also been evaluated with the pseudo-second-order rate constants. The values of E_a for AB25 on CPB in the presence and in absence of ultrasound, respectively, are 20.14 and 25.80 kJ/mol, which confirm that the process is physical nature (E_a < 40 kJ/mol) both with and without the assistance of ultrasound. This was further confirmed by the values of $\Delta H°$ obtained. Additionally, the biosorbent surface was characterized by surface-specific area, isoelectric potential (pH_{ZPC}), surface functional groups, and scanning electron microscopy.

Keywords: Ultrasonic irradiation; Biosorption; Cycads palm bark; Acid blue 25; Kinetics; Characterization

1. Introduction

Pollutants discharged from various industries are creating a threat to the Earth's biodiversity. Water pollution is of major concern among the various types of environmental pollutions. Dye-based industries are one of the major causes of this pollution because the dyes wasted by these industries are the main source of water pollution [1]. The presence of small amounts of dyes in water is greatly adverse and their carcinogenic and mutagenic potentials could origin dangerous effects on the fauna and the flora beings by direct or indirect utilization. Dyes can be classified as anionic (direct, acid, and reactive dyes), cationic (basic dyes), and non-ionic (disperse dyes) [2]. Acid dyes are organic sulphonic acids; the commercially available forms are usually sodium salts, which exhibit good water solubility. In a sequence of their importance, acid dyes are mostly used with certain fiber types such as polyamide, wool, silk, modified acrylic, and polypropylene fibers, as well as blends of the aforementioned fibers with other fibers such as cotton, rayon, polyester, regular acrylic, etc. [3]. Acid blue 25, an anionic anthraquinonic dye, was chosen as a typical representative pollutant. Various

* Corresponding author.

methods exist for the removal of dyes from solution; however, these methods are expensive mainly in developing countries from the viewpoint of economics. The study of biosorption which utilizing natural materials or industrial and agricultural wastes is of great importance from an environmental point of view, as it can be considered as an alternative technique for removing toxic pollutants from Guechi and Benabdesselam [4], Rangabhashiyam et al. [5], Guechi and Hamdaoui [6,7], Silva et al. [8], El-Sayed [9], and Guechi [10]. Cycads palm (Cycadaceae family) are seed plants typically characterized by a stout and woody (ligneous) trunk with a crown of large, hard and stiff, evergreen leaves. They usually have pinnate leaves. Cycads palm vary in size from having trunks only a few centimeters to several meters tall and are found across much of the subtropical and tropical parts of the world. It has a rosette of pinnate leaves around the cylindrical trunk.

Thus, the aim of the present study is to characterize the cycads palm bark (CPB) and to investigate the potential of this as a novel biosorbent for the removal of AB25 from aqueous media in a batch process in the absence and presence of ultrasonic irradiation. Ultrasound is a green technology because it requires no additional chemicals and only involves sound energy [11]. Several physical, chemical, and mechanical effects can result when a liquid suspension of solid particles is subjected to the action of ultrasound. Ultrasonic waves strongly affect mass transfer between two phases. It is well-understood that ultrasonic waves have a greater efficiency for interface mixing than conventional (classical) agitation [12]. This behavior could be the motive for the improvement of the sorption kinetic process [13–16]. Also, ultrasound waves cause cavitation in liquid, involving the formation of small bubbles, growth, and collapse due to pressure fluctuation [16]. Different cavitation bubbles that subside not uniformly unevenly near the solid surface will generate a microjet that was able to transform the particle size of sorbent and its morphology.

2. Materials and methods

2.1. Preparation and characterization of biosorbent

The waste CPB was collected after they pruned these trees on the campus of our university in Annaba (east of Algeria) and washed them with distilled water several times to remove dust and other materials. The CPB was crushed and sieved to desired mesh size (0.16–1.25 mm). After, the material was washed for the second time, and then completely dried in an oven at 60°C for 5 d. Finally, the obtained material was stored in desiccators until use.

The surface functional groups of this biosorbent were determined by the Boehm method and using a (SHIMADZU FTIR-8400S) Fourier transform infrared spectrometer (FTIR) analysis, in which the spectra were recorded from 4,000 to 400 cm^{-1} by preparing KBr pellets for sample preparation. The isoelectric potential or point of zero charges (pHpzc) of the CPB characteristics was determined by using the solid addition method [7,8]. In addition, scanning electron microscopy (SEM) analysis was carried out on the CPB to study the morphology of the CPB surface, and the specific surface area (SSA) was determined using an alternative method to the Bruner–Emmet–Teller (BET) method [7,17].

2.2. Chemicals

The acid blue 25 (Telon Blue ANL) (C.I. 62055) (Sigma-Aldrich, Algeria), is an anionic acid dye of the anthraquinone chemical class dye, [molecular formula $C_{20}H_{13}N_2NaO_5S$, FW 416.39 g/mol, λ_{max} 603 nm (measured value)]. The chemical structure of the dye used in the experiments is shown in Fig. 1.

Three hundred milligram per liter stock solution was prepared by dissolving the required amount of each dye in distilled water. 0.1 N H_2SO_4 and 0.1 N NaOH solutions used for the pH adjustment were prepared by using concentrated H_2SO_4 and NaOH (Merck, reagent grade) solutions, respectively. Working solutions of the desired concentrations were obtained by successive dilutions.

2.3. Experimental setup

Batch biosorption experiments were carried out in the experimental setup shown in Fig. 2 [18]. The set-up consisted of an ultrasonic cleaning bath operating at a frequency of 40 kHz with an electrical nominal output power of 250 W. Acoustic power dissipated in the medium was measured by the calorimetric method [19]. Batch biosorption experiments were carried out by adding 0.15 g of CPB to 50 mL of AB25 solution in a conical flask with an initial dye concentration range of 5–25 mg/L and the temperature was controlled at 25°C ± 2°C. The temperature in the ultrasonic bath was fixed by recirculation water (Fig. 2).

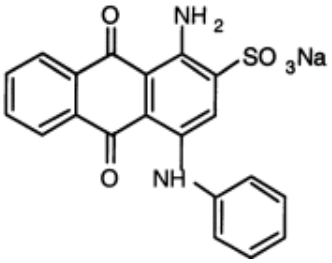

Fig. 1. Chemical structure of acid blue 25 dye.

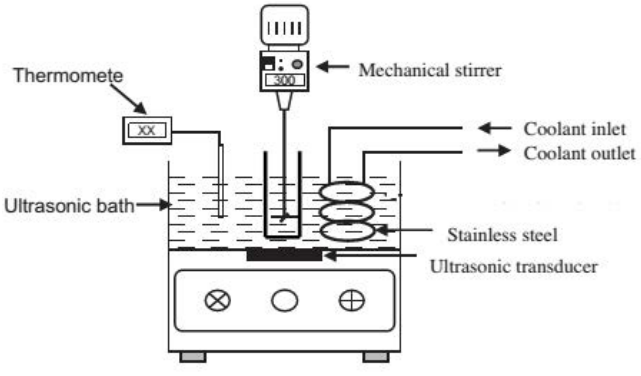

Fig. 2. Experimental setup in this study [18].

The mixture was stirred at a fixed stirring speed of 300 rpm (absence of ultrasound) or in presence of ultrasound without agitation. In a preliminary kinetic test under these conditions by applying the highest (25 mg/L) AB25 dye concentration, it was established that the equilibrium was reached at 150 min in presence of US and at 210 min for agitation only. For sure, all kinetic experiments, aqueous samples were taken lasted equilibrium time (300 min) for each case. At predetermined intervals of time, samples were taken from the flask were centrifuged (3,000 rpm for 10 min) and after the concentrations were analyzed by using a double beam UV-vis spectrophotometer (UV-6405, Jenway) at the maximum wavelength (603 nm). The samples were reintroduced after analysis so that the volume of the solution remained constant during the course of the kinetics. Each experiment was duplicated under identical conditions. The amount of biosorption at time t, q_t (mg/g), and the % removal of AB25 dye were calculated by the following equations:

$$q_t = \frac{(C_0 - C_t)V}{W} \quad (1)$$

$$\%\ \text{removal} = \frac{C_0 - C_t}{C_0} \times 100 \quad (2)$$

where C_0 and C_t (mg/L) are the initial concentrations of dye and the dye concentration of solution at time t, respectively. V is the volume of dye solution (L) and W is the mass of dry biosorbent used (g).

3. Results and discussion

3.1. Influence of operating conditions

3.1.1. Effect of solution pH

Previous studies have shown that pH has an important role in the biosorption process [10,20–24]. Because of this fact, several assays with different pH values have been carried out, varying the initial pH of solutions between 2 and 8 for the biosorption AB25 dye by CPB in the absence and presence of ultrasound. It can be seen that the result from the Fig. 3 reveals that the kinetics of the percentage removal of AB25 dye decreased from 67.79% to 24.64% in absence of ultrasound and from 95.73% to 27.69% in presence of ultrasound whiles the pH of the solution increase from 2.0 to 8.0, respectively. As, pH of the system decreased, the number of positively charged surface sites increased and the number of negatively charged biosorption sites decreased, which favorite the biosorption of negatively charged dye anions of AB25 due to electrostatic attraction. But at pH of the system increased the number of negatively charged surface sites increased and the number of positively charged biosorption sites increased, which unfavorably the biosorption negatively charged dye anions of AB25 due to electrostatic repulsion. Consequently, the low pH favorably for the biosorption of AB25 as an anionic dye in the presence of ultrasound and only stirring (classic method) and the optimum pH in this study was 2.0.

It was shown that the percentages of AB25 dye removal to be greater in the presence of ultrasound than with only stirring (classical method) because it is well-understood that ultrasonic waves have a greater efficiency for interface mixing than classical (stirring alone).

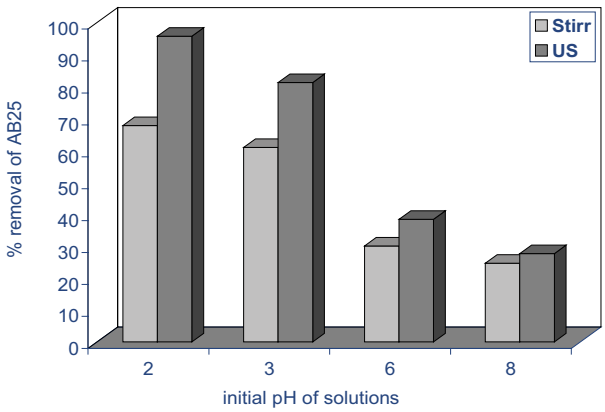

Fig. 3. Effect of initial pH of solution on the percentage removal of AB25 dye in presence and in absence of ultrasound (conditions: C_0: 25 mg/L; V: 50 mL; stirring speed: 300 rpm; T: 25°C; pH: 2–8).

3.1.2. Effect of contact time and initial dye concentration

The initial dye concentration in the solution plays a key role as a driving force to overcome the mass transfer resistance between the solution and solid phases. Fig. 4 shows the effect of different initial dye concentrations of AB25 at pH 2 and a biosorbent dosage of 0.15 g/50 mL as a function of contact time in the presence and absence of ultrasound. The plots showed that the amount of AB25 biosorbed for both cases (ultrasonic and classic) increase with time till it reached a constant value beyond which no more dye was further removed from the solution. These plots illustrate that both methods can be devised into three distinct regions (stages): at first, rapid biosorption, following slowed downstage till the equilibrium state for each temperature and at the third stage, the biosorption achieving equilibrium. An increase in initial dye concentration leads to an increase in the amount biosorbed of AB25 (Fig. 4), this is due to increasing concentration gradient, which acts as an increasing driving force to overcome all mass transfer resistances between the aqueous solution and solid phase [6]. For all initial dye concentrations, the biosorption of AB25 on CPB was faster and higher in the presence of ultrasound than in its absence (Fig. 4). The improvement of sorption by sonication may be explained by the intensification of mass transfer phenomena and thermal effects of ultrasound [16]. Furthermore, the asymmetric collapse of bubbles in a heterogeneous system produces micro-jets with high rapidity on the surface of the biosorbent. This act leads to destroy and tear off the biosorbent which may possibly representation new sites and increase the internal biosorption capacity and moreover pretty mass transfer into the pores. These effects can be reasons for increasing the biosorption capacity in the presence of ultrasound and the biosorbent reached an equilibrium state in a short period.

When initial dye concentration was increased from 5 to 25 mg/L, the amount biosorbed at equilibrium increased

from 1.03 to 4.84 mg/g by the classical method and from 1.38 to 6.09 mg/g by sonication method. Furthermore, Fig. 4 reveals that the contact time of AB25 biosorption on CPB for both methods, required to reach the equilibrium at initial concentrations from 5 to 25 mg/L, was from 40 to 150 min and from 50 to 210 min, respectively, with sonicated and unsonicated (classical).

3.1.3. Effect of biosorbent dose

The batch equilibrium studies at different CPB dose values were carried out in the range of 0.15–0.7 g/50 mL. The experiments were carried out at 25 mg/L initial dye concentration with pH (2) at 25°C ± 2°C for equilibrium time and a constant stirring speed of 300 rpm. Fig. 5 illustrates the effect of biosorbent dose on the biosorption of AB25 dye in the presence and in absence of ultrasound. The amount of AB25 biosorbed per unit mass of biosorbent decreases with an increase in biosorbent dose due to the concentration gradient between solute concentrations in the solution and on the biosorbent surface [7]. The amount biosorbed of AB25 dye decreased from 4.84 to 1.01 mg/g in absence of ultrasound and from 6.09 to 1.39 mg/g in presence of ultrasound whiles the biosorbent dose increase from 0.15 to 0.7 g, respectively. In contrast, the results (figure not shown) indicate that an increase in the biosorbent dose resulted in increase in the percentage removal of AB25 is due to the increase in the number of biosorption sites.

For all biosorbent dosages (Fig. 5), it was observed that biosorption was less effective in the absence than in the presence of ultrasound. Also, the biosorption of AB25 dye needs more time higher with ultrasound than in absence of ultrasound. This could be related to the higher mass transport in the presence of the ultrasound. Microjets and shockwaves produced by the cavitation can disturb the structure of the sorbate and lead to a higher biosorption capacity [25]. Similar results have been reported for the removal of malachite green dye by dead pine needles [16].

3.1.4. Effect of temperature

Temperature is a highly significant parameter in the biosorption processes. For estimation of temperature was carried for testing the aptitude of CPB in the presence and absence of ultrasound (Fig. 6). The biosorption capacity of CPB increased with increasing temperature in both cases.

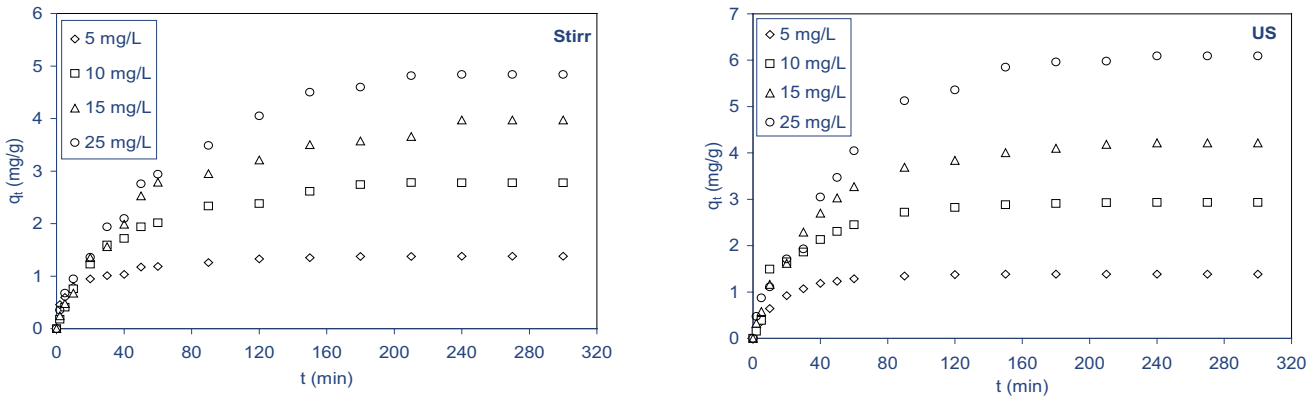

Fig. 4. Effect of initial concentration and contact time on the removal of AB25 dye vs. time in presence and in absence of ultrasound (conditions: C_0: 5–25 mg/L; V: 50 mL; stirring speed: 300 rpm; T: 25°C; pH: 2).

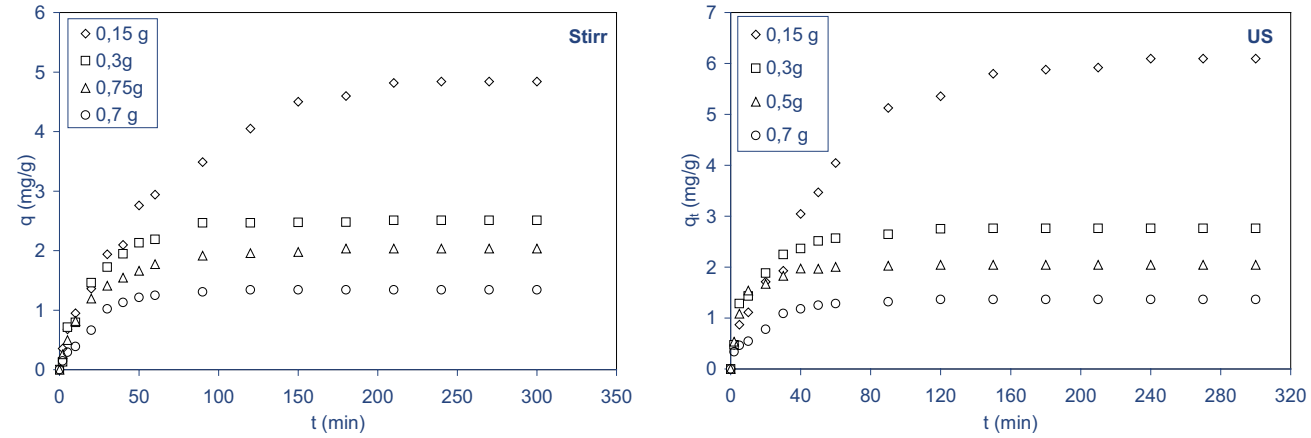

Fig. 5. Effect of biosorbent dosage on the removal of AB25 dye vs. time in presence and in absence of ultrasound (conditions: C_0: 25 mg/L; V: 50 mL; stirring speed: 300 rpm; T: 25°C; pH: 2).

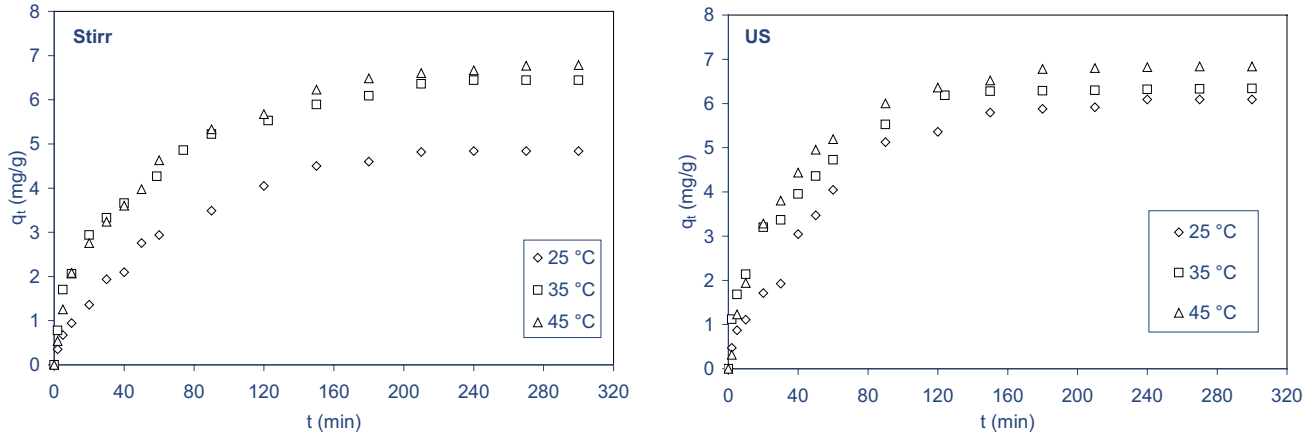

Fig. 6. Effect of temperature on the removal of AB25 dye vs. time in presence and in absence of ultrasound (conditions: C_0: 25 mg/L; V: 50 mL; stirring speed: 300 rpm; T: 25°C–45°C; pH: 2).

This indicates that the biosorption process was endothermic in nature. The amount of biosorption at equilibrium increased from 4.84 to 5.48 mg/g in the absence of ultrasound and from 6.09 to 6.84 mg/g in the presence of ultrasound when the temperature was increased from 25°C to 45°C. It was explained that as temperature increased, the mobility of AB25 dye increased which caused to increase in the rate of diffusion of the sorbate molecules across the boundary layer and in the internal pores of the particle CPB. In addition, in the presence of ultrasound, the cavitation process may be the surface area changes of biosorbent (morphology) and some new active sites might be produced, which lead to elevated rate biosorption.

3.1.5. Effect of biosorbent particle size

Fig. 7 shows the percentage removal of AB25 dye at three different particle sizes in the absence and presence of irradiation ultrasonic. It was observed from this figure, the % removal is enhanced as the particle size decreases for both methods. The percentage removal of acid dye decreases from 90%, 01% to 32.34% mg g^{-1} and from 97.87% to 40.54% in the absence and in presence of irradiation ultrasonic, respectively, with an increase in particle size of CPB from 0.16 to 1.25 mm. This is because the smaller particles have more surface area and access to the particle pores is facilitated when their size is small. It was observed that the percentage removal of AB25 was higher in the presence of ultrasound irradiation than stirring, and this is due to the asymmetrically collapse of bubbles which lead to the breaking of large particles to form smaller ones opens some tiny sealed channels that are to say change the size and morphology of the surface, which might then become available for biosorption. So, ultrasonic waves can increase the surface area and also the mass transfer which both lead to a higher biosorption process [13,26].

3.2. Batch biosorption kinetic

The experimental results for different initial temperature solutions for the biosorption kinetics of AB25

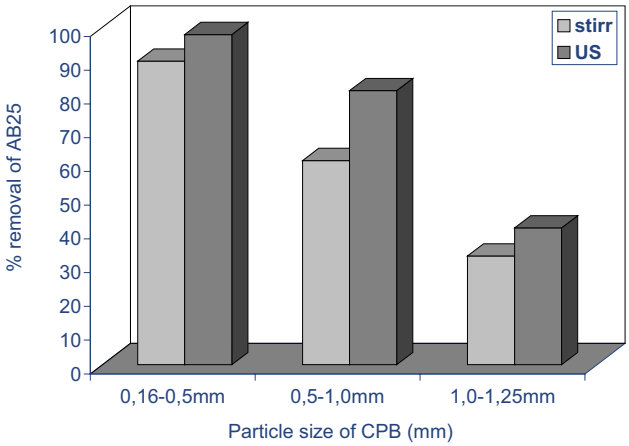

Fig. 7. Effect of particle size on the percentage removal of AB25 dye in presence and in absence of ultrasound (conditions: C_0: 25 mg/L; V: 50 mL; stirring speed: 300 rpm; T: 25°C; pH: 2).

by CPB were modeled by the pseudo-first-order [27] and pseudo-second-order [7,14] in presence and in absence of ultrasound.

Lagergren equation was used to investigate the suitability of pseudo-first-order kinetic model to describe the adsorption process. This equation of this model can be written as:

$$\ln(q_e - q_t) = -k_1 t + \ln q_e \quad (3)$$

where q_e (mg/g) and q_t (mg/g) represent the biosorbed amount of AB25 at equilibrium and at any time t, respectively, and k_1 (min^{-1}) is the rate constant for Lagergren-first-order model.

The plot of $\ln(q_e - q_t)$ vs. t gives a straight line for the pseudo-first-order biosorption kinetics at different temperatures in the presence and in absence of ultrasound (figure not shown). The slope of the plot was used to determine the equilibrium rate constant, k_1, and the intercept for the biosorption at equilibrium, $q_{e,cal}$. The k_1 values, the

correlation coefficients, the calculated biosorbed amount ($q_{e,cal}$), and experimental ($q_{e,exp}$) values were regrouped in Table 1. As seen in this Table 1, both cases are based on the correlation coefficients ($r \geq 0.956$) values obtained were low, subsequently, the results confirm that were not appropriate to use the pseudo-first-order kinetic model to predict the biosorption kinetics of AB25 dye on CPB.

Pseudo-second-order model has been frequently employed to analyze biosorption data obtained from various experiments using different adsorbates and biosorbents [7,10,20,25,28,29]. The pseudo-second-order kinetic model is based on the sorption equilibrium capacity of the solid phase and can be expressed as:

$$\frac{t}{q_t} = \frac{1}{k_2 q_e^2} + \frac{1}{q_e} t \tag{4}$$

$$h = k_2 q_e^2 \tag{5}$$

where k_2 (g/mg min) is the rate constant for the pseudo-second-order sorption kinetics, q_e (mg/g) and q_t (mg/g) are the amount biosorbed at equilibrium and at any time t, respectively, and h (min/mg g) is the initial sorption rate.

Table 1 shows the pseudo-second-order kinetic parameters for different temperatures of AB25 dye obtained by utilizing the linear regression analysis method. For both methods (sonication and classical), the experimental data showed a good agreement with the pseudo-second-order equation because the correlation coefficients for the linear plots were high (≥0.996) at all the studied temperatures and for the entire period (Fig. 8).

In addition, the calculated $q_{e,cal}$ values agree with the experimental data for each method. These results suggested that the experimental data for the biosorption kinetics for AB25 by CPB were adequately represented by the pseudo-second-order kinetic model for the entire period and for all temperature studies.

3.3. Estimation of activation energy

The activation energy (E_a) is defined as the minimum kinetic energy required by the biosorbate ions to react with the active sites available on the surface of the biosorbent [30]. As the pseudo-second-order kinetic model was adjudged the best for the biosorption of AB25 on CPB in the presence and in absence of ultrasound, then the pseudo-second-order kinetic rate constant, k_2, was used to determine the activation

Table 1
Parameters of the kinetic models for the biosorption of AB25 on CPB at different temperatures

Model	Classical method (stirring)			Ultrasound method		
Pseudo-first-order	25°C	35°C	45°C	25°C	35°C	45°C
$q_{e,exp}$ (mg/g)	4.84	5.05	5.48	6.09	6.34	6.84
$q_{e,cal}$ (mg/g)	5.83	6.58	6.89	6.03	7.47	6.01
k_1 (min^{-1})	0.0293	0.0204	0.0121	0.0402	0.0277	0.0209
r	0.956	0.976	0.977	0.983	0.959	0.973
Pseudo-second-order						
k_2 (g/mg min)	0.013	0.019	0.025	0.003	0.004	0.005
$q_{e,cal}$ (mg/g)	4.81	5.35	5.52	6.32	6.41	6.40
h (mg/g min)	0.110	0.217	0.261	0.144	0.272	0.282
r	0.996	0.999	0.998	0.997	0.997	0.998

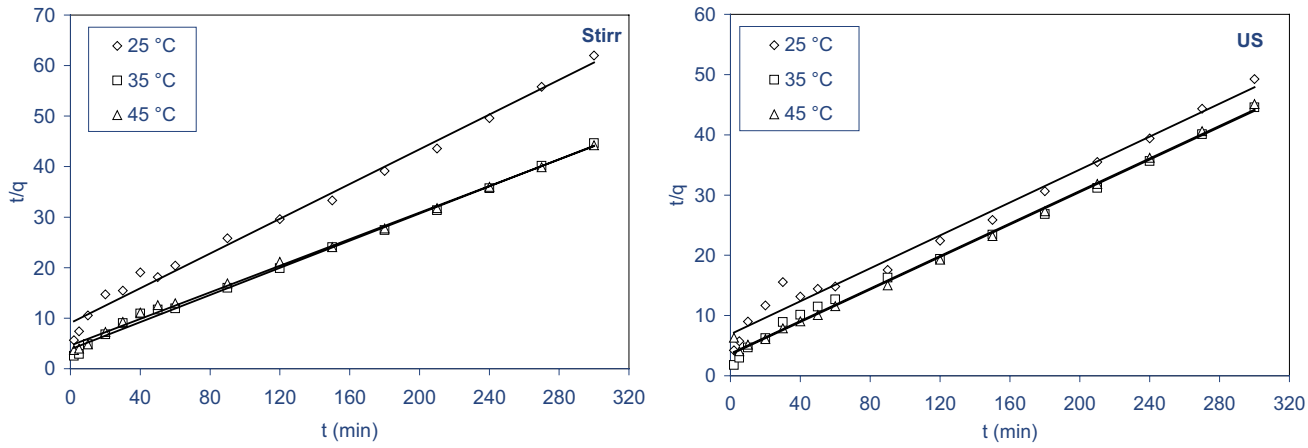

Fig. 8. Linear plots of pseudo-second-order model for the biosorption of AB25 in presence and in absence of ultrasound.

energy (E_a) of the adsorption, using the Arrhenius equation (Eq. (6)) [25,29,31]:

$$\ln k_2 = \ln A - \frac{E_a}{RT} \quad (6)$$

where k_2 is the pseudo-second-order kinetic rate constant, E_a is the Arrhenius activation energy of adsorption (kJ/mol), A is the Arrhenius factor (g/mg min), R is the gas constant (8.314 J/mol K), and T (K) is the absolute temperature of the solution.

The slope of the plot of $\ln k_2$ vs. $1/T$ is used to evaluate the activation energy for the biosorption of AB25 by CPB in the absence and in presence of ultrasound (Fig. 9). Activation energy is often used as the basis to differentiate between physically and chemically controlled processes, in which the physisorption processes frequently have energies in the range of 5–40 kJ/mol, while higher activation energies (40–800 kJ/mol) describe the chemisorptions [32]. Therefore, the values of E_a for AB25 on CPB in the presence and in absence of ultrasound, respectively, is 20.14 and 25.80 kJ mol^{-1}, that is, <40 kJ mol^{-1} proves the physical nature of this biosorption process. This difference could be attributed to the effect of ultrasound on the sorbent, because, ultrasound gives to the medium a lot of energy, leading to the reduction of the potential barrier of sorption and therefore requires reduced activation energy [25]. Similar observations have been reported in the literature [33–35].

In a characteristic sorption study, a necessary decision has to be made on whether the reaction is physical or chemical in nature and spontaneous or not; based on thermodynamic parameters such as a change in enthalpy ($\Delta H°$), entropy ($\Delta S°$), and Gibbs free energy ($\Delta G°$). The parameters were determined using the following relations:

$$\Delta G° = -R_g T \ln b \quad (7)$$

$$\Delta G° = \Delta H° - T\Delta S° \quad (8)$$

where T (K) is the absolute temperature and R_g is the gas constant, and b (L/mol) is the Langmuir equilibrium constant.

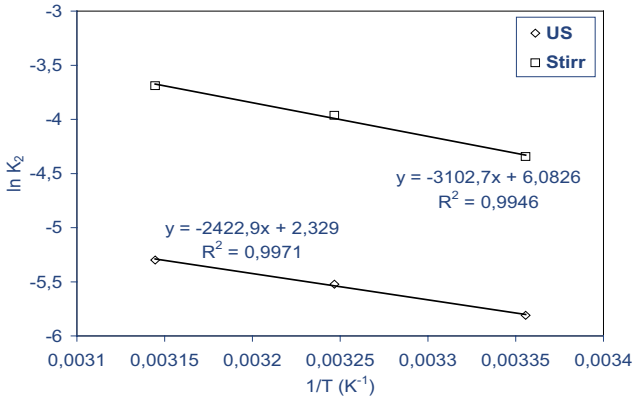

Fig. 9. Plot of $\ln k_2$ vs. $1/T$ for the biosorption of AB25 in presence and in absence of ultrasound.

By using Eq. (7), free energy change ($\Delta G°$) values were calculated at different temperatures and a plot of $\Delta G°$ against T gives a graph (figure not shown) where we can obtain $\Delta H°$ from the intercept and $\Delta S°$ from the slope (Eq. (8)). A plot of $\Delta G°$ vs. T was found to be linear with the determination coefficient (R^2) was found to be 0.998 and 0.987 in the presence and in absence of ultrasound, respectively. The thermodynamic parameters obtained at various temperatures in the presence and in absence of ultrasound are presented in Table 2. The negative values obtained for change of Gibbs free energy ($\Delta G°$), reveal the feasibility of the process and the spontaneous nature for the biosorption of AB25 by CPB. Knowing that generally, the change of free energy for the physical and chemical adsorption is in the range of 0 to −20 kJ/mol and −80 to−400 kJ/mol, respectively [36]. The positive values of enthalpy ($\Delta H°$) obtained at all temperatures indicating the biosorption process was endothermic, physical in nature, and involves strong forces between the active sites on the CPB and the AB25 dye species and also between adjacent AB25 dye on the biosorbed phase [37]. The low and positive value of entropy ($\Delta S°$) at all temperatures under study indicates that may imply that no remarkable change in entropy occurred during the biosorption of AB25 dye and showed and also showed affinity between the adsorbent and adsorbate [38,39] both with and without the assistance of ultrasound. In the literature, similar results of the thermodynamic parameters were reported [25].

3.4. Characterization of CPB as biosorbent

Some physicochemical properties of CPB are collected in Table 3. The isoelectric potential (pHzpc) of CPB characteristics was done by using the solid addition method [7,40]. The initial pH (pH_i) of the prepared KNO_3 solution (0.1 N) was adjusted between 2 and 12. After, 1 g of biosorbent was added to each solution and the samples were stirred at slowly agitation for 48 h, then the final pH (pH_f)

Table 2
Thermodynamic parameters for the biosorption of AB25 by CPB

Thermodynamic parameters	$\Delta H°$ (kJ/mol)	$\Delta S°$ (kJ/mol)	$-\Delta G°$(kJ/mol)		
			298 K	308 K	318 K
Stirring	3.01	29.5	5.81	6.04	6.4
Ultrasound	1.42	22.3	5.68	5.80	5.95

Table 3
Principal characteristics of cycads palm bark

Parameters	Value
Apparent specific gravity	0.36
Absolute specific gravity	1.33
Point of zero charge (pH_{PZC})	4.9
Porosity (%)	72.93
Mean diameter (mm)	≤1.25

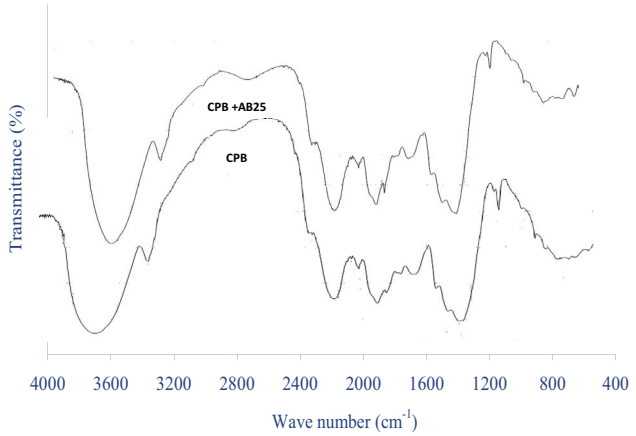

Fig. 10. FTIR spectra of cycads palm bark before and after biosorption of AB25.

Table 4
Concentrations of surface functionality of cycads palm bark

Concentration of acidic and basic groups on CPB surface	mequiv/g
Carboxylic	0.02
Lactonic	0.07
Phenolic	1.47
Carbonylic and quinonic groups	2.26
Acidic groups total	3.82
Basic groups total	0.84

of the solutions was measured. The value of pH_{ZPC} can be determined from the curve that crosses the initial pH value lines of the plot ($pH_i - pH_f$) vs. pH_i (figure not shown). So, the result of pH_{zpc} was measured to be 4.9 and it was noted in Table 3.

The FTIR spectra obtained (Fig. 10) revealed that there are various functional groups detected on the surface of CPB. It can be seen peaks are assigned the OH stretch of water (3,687 cm^{-1}) group, the elongation of OH the phenol of cellulose or lignin (3,460 cm^{-1}), to the presence of CH_2 aliphatic of cellulose (2,920 cm^{-1}), to the presence of C=O group of ketones or aldehydes and amides (1,733 cm^{-1}), the C=C stretching of the phenol group (1,612 cm^{-1}), to the CH_3 deformation (1,384 cm^{-1}), the C–N stretching (1,190 cm^{-1}), to the stretching of the SO_2 (875 cm^{-1}) and C–O–H twists (663). The FT-IR spectrum after AB25 dye biosorption, shown in Fig. 10, indicates that the peaks due to the above functional groups are slightly affected in their position and intensity, which indicated that the functional groups on the surface of CPB participated in the AB25 biosorption.

The Boehm method (Table 4) quantitatively proved these results. These results show that several types of surface groups. From acid groups, show absence of carboxylic groups, the carbonylic, the quinonic, and the phenolic groups were the dominant acidic oxygenated groups.

As an alternative to the BET method, the SSA (m^2/g) of the CPB uses the following equation (Eq. (9)) [7,20,41]:

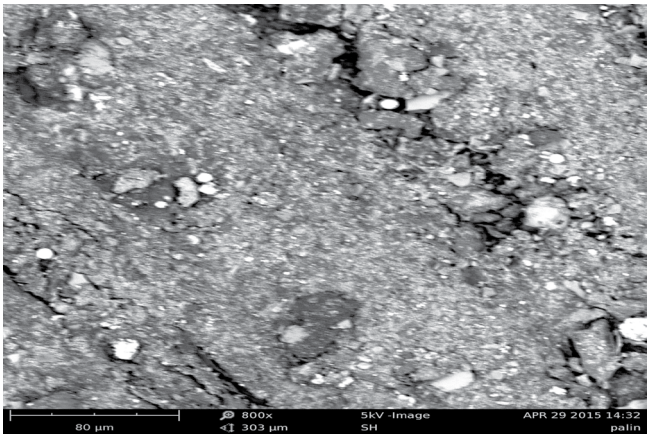

Fig. 11. SEM image of particle morphology (800× magnifications) of CPB samples.

$$SSA = \frac{F \cdot q_m \cdot N_{AV} \cdot A}{MW \cdot 10^3} 10^{-20} \quad (9)$$

where SSA is the specific surface area (m^2/g of sorbent), F is the fraction dye in the commercial product (0.45), q_m is the monolayer capacity (g dye/g solid) from the Langmuir model, is calculated in the absence and in presence of ultrasound, respectively, to 22.03 and 30.99 mg/g. N_{AV} is the Avogadro number (6.022×10^{23} molecules/mol), MW is the molecular weight of the dye (416.39 g/mol) and A is the molecular area of the dye (m^2). The molecular area of AB25 was taken as 80 $Å^2$ [41]. According to Eq. (9), the SSA of CPB was found 11.47 and 16.13 m^2/g, respectively in absence and in presence of ultrasound.

In addition, the scanning electron micrograph (SEM) of raw CPB sample at bar length equivalent to 80 µm, working voltage 5 kV with 800× magnification is shown in Fig. 11. This Fig. 11 reveals that the CPB a rough, opaque, and porous surface morphology.

4. Conclusions

The removal of AB25 dye from aqueous media by CPB was appreciably enhanced in the presence of ultrasound. The optimum pH for biosorption was 2.0 and the maximum AB25 biosorption capacity was found to be greater in the presence than in the absence of ultrasound, contrary to equilibrium state period for biosorption. The biosorption kinetic data were found to be well-represented by the pseudo-second-order rate equation, both in the absence and presence of ultrasound. The values of E_a for AB25 on CPB in the presence and in absence of ultrasound, respectively, are 20.14 and 25.80 kJ/mol proves the physical nature of this biosorption process. This was also confirmed by the low value of enthalpy ($\Delta H°$) obtained.

Acknowledgments

This study was supported by the Ministry of Higher Education and Scientific Research of Algeria (project No. A16N01UN230120180002) through the General Directorate of Scientific Research and Technological Development (GD-SRTD).

References

[1] T.E. Kose, Agricultural residue anion exchanger for removal of dyestuff from wastewater using full factorial design, Desalination, 222 (2008) 323–330.
[2] I.D. Mall, V.C. Srivastava, N.K. Agarwal, Removal of Orange-G and Methyl Violet dyes by adsorption onto bagasse fly ash—kinetic study and equilibrium isotherm analyses, Dyes Pigm., 69 (2006) 210–223.
[3] A.A. Attia, W.E. Rashwan, S.A. Khedr, Capacity of activated carbon in the removal of acid dyes subsequent to its thermal treatment, Dyes Pigm., 69 (2006) 128–136.
[4] E.-K. Guechi, S. Benabdesselam, Removal of cadmium and copper from aqueous media by biosorption on cattail (*Thypha angustifolia*) leaves: kinetic and isotherm studies, Desal. WaterTreat., 173 (2020) 367–382.
[5] S. Rangabhashiyam, E. Nakkeeran, N. Anu, N. Selvaraju, Biosorption potentials of a novel *Ficus auriculata* leaves powder for the sequestration of hexavalent chromium from aqueous solutions, Res. Chem. Intermed., 41 (2015) 8405–8424.
[6] E.K. Guechi, O. Hamdaoui, Cattail leaves as a novel biosorbent for the removal of malachite green from liquid phase: data analysis by non-linear technique, Desal. Water Treat., 51 (2013) 3371–3380.
[7] E.K. Guechi, O. Hamdaoui, Biosorption of methylene blue from aqueous solution by potato (*Solanum tuberosum*) peel: equilibrium modelling, kinetic, and thermodynamic studies, Desal. Water Treat., 57 (2016) 10270–10285.
[8] L.S. Silva, L.C.B. Lima, F.C. Silva, J.M.E. Matos, M.R.M.C. Santos, L.S.S. Junior, K.S. Sousa, E.C. Silva Filho, Dye anionic sorption in aqueous solution onto a cellulose surface chemically modified with amino ethanethiol, Chem. Eng. J., 218 (2013) 89–98.
[9] G.O. El-Sayed, Removal of methylene blue and crystal violet from aqueous solutions by palm kernel-fiber, Desalination, 272 (2011) 225–232.
[10] E.K. Guechi, Equilibrium, kinetics and mechanism for the removal of Rhodamine B by adsorption on Okoume (*Aucoumea klaineana*) sawdust from aqueous media, Desal. Water Treat., 94 (2017) 164–173.
[11] X. Wang, A. Wang, J. Ma, M. Fu, Facile green synthesis of functional nanoscale zero valent iron and studies of its activity toward ultrasound-enhanced decolorization of cationic dyes, Chemosphere, 166 (2017) 80–88.
[12] M.H. Entezari, A. Keshavarzi, Phase-transfer catalysis and ultrasonic waves. II. Saponification of vegetable oil, Ultrason. Sonochem., 8 (2001) 213–216.
[13] M. Breitbach, D. Bathen, Influence of ultrasound on adsorption processes, Ultrason. Sonochem., 8 (2001) 277–283.
[14] O. Hamdaoui, E. Naffrechoux, L. Tifouti, C. Petrier, Effects of ultrasound on adsorption–desorption of p-chlorophenol on granular activated carbon, Ultrason. Sonochem., 10 (2003) 109–114.
[15] G. Zhang, P. Zhang, B. Wang, H. Liu, Ultrasonic frequency effects on the removal of *Microcystis aeruginosa*, Ultrason. Sonochem., 13 (2006) 446–450.
[16] O. Hamdaoui, M. Chiha, E. Naffrechoux, Ultrasound-assisted removal of malachite green from aqueous solution by dead pine needles, Ultrason. Sonochem.,15 (2008) 799–807.
[17] B.H. Hameed, M.I. El-Khaiary, Batch removal of malachite green from aqueous solutions by adsorption on oil palm trunk fibre: equilibrium isotherms and kinetic studies, J. Hazard. Mater., 154 (2008) 237–244.
[18] C. Djelloul, A. Hasseine, Ultrasound-assisted removal of methylene blue from aqueous solution by milk thistle seed, Desal. Water Treat., 51 (2013) 5805–5812.
[19] P.R. Gogate, I.Z. Shirgaonkar, M. Sivakumar, P. Senthilkumar, N.P. Vichare, A.B. Pandit, Cavitation reactors: efficiency assessment using a model reaction, AIChE J., 47 (2001) 2526–2538.
[20] F. Ferrero, Dye removal by low cost adsorbents: hazelnut shells in comparison with wood sawdust, J. Hazard. Mater., 142 (2007) 144–152.
[21] M.C. Ncibi, B. Mahjouba, M. Seffen, Kinetic and equilibrium studies of methylene blue biosorption by *Posidonia oceanica* (L.) fibres, J. Hazard. Mater., 139 (2007) 280–285.
[22] S.K. Low, M.C. Tan, Dye adsorption characteristic of ultrasound pre-treated pomelo peel, J. Environ. Chem. Eng., 6 (2018) 3502–3509.
[23] J. Shah, M. Rasul Jan, A. Haq, Y. Khan, Removal of Rhodamine B from aqueous solutions and wastewater by walnut shells: kinetics, equilibrium and thermodynamics studies, Front. Chem. Sci. Eng., 7 (2013) 428–436.
[24] I. Chaari, E. Fakhfakh, M. Medhioub, F. Jamoussi, Comparative study on adsorption of cationic dyes by smectite rich natural clays, J. Mol. Struct., 1179 (2019) 672–677.
[25] L. Nouri, O. Hamdaoui, Ultrasonication-assisted sorption of cadmium from aqueous phase by wheat Bran, J. Phys. Chem., 111 (2007) 8456–8463.
[26] M.H. Entezari, N. Ghows, M. Chamsaz, Ultrasound facilitates and improves removal of Cd(II) from aqueous solution by the discarded tire rubber, J. Hazard. Mater., 131 (2006) 84–89.
[27] S. Lagergren, B.K. Svenska, On the theory of so-called adsorption of dissolved substances, The Royal Swedish Academy of Sciences Document, Band, 24 (1898) 1–13.
[28] M. Dogan, Y. Ozdemir, M. Alkan, Adsorption kinetics and mechanism of cationic methyl violet and methylene blue dyes onto sepiolite, Dyes Pigm., 75 (2007) 701–713.
[29] Y.S. Ho, G. McKay, Sorption of dye from aqueous solution by peat, Chem. Eng. J., 70 (1998) 115–124.
[30] A.A. Jalil, S. Triwahyono, M.R. Yaakob, Z.Z.A. Azmi, N. Sapawe, N.H.N. Kamarudin, H.D. Setiabudi, N.F. Jaafar, S.M. Sidik, S.H. Adam, B.H. Hameed, Utilization of bivalve shell-treated *Zea mays* L. (maize) husk leaf as a low-cost biosorbent for enhanced adsorption of malachite green, Bioresour. Technol., 120 (2012) 218–224.
[31] B.H. Hameed, A.A. Ahmad, N. Aziz, Isotherms, kinetics and thermodynamics of acid dye adsorption on activated palm ash, Chem. Eng. J., 133 (2007) 195–203.
[32] M. Dogan, M. Alkan, O. Demirbas, Y. Ozdemir, C. Ozmetin, Adsorption kinetics of maxilon blue GRL onto sepiolite from aqueous solutions, Chem. Eng. J., 124 (2006) 89–101.
[33] B.S. Schueller, R.T. Yang, Ultrasound enhanced adsorption and desorption of phenol on activated carbon and polymeric resin, Ind. Eng. Chem. Res., 40 (2001) 4912–4918.
[34] O. Hamdaoui, R. Djeribi, E. Naffrechoux, Desorption of metal ions from activated carbon in the presence of ultrasound, Ind. Eng. Chem. Res., 44 (2005) 4737–4744.
[35] Y. Shimizu, R. Yamamoto, H. Shimizu, Effects of ultrasound on dyeing of Nylon 6, Text. Res. J., 59 (1989) 684–687.
[36] A. Ozer, G. Akkaya, M. Turabik, Biosorption of Acid Blue 290 (AB 290) and Acid Blue 324 (AB324) dyes on *Spirogyra rhizopus*, J. Hazard. Mater., 135 (2006) 355–364.
[37] I.A.W. Tan, A.L. Ahmad, B.H. Hameed, Adsorption of basic dye on high-surface-area activated carbon prepared from coconut husk: equilibrium, kinetic and thermodynamic studies, J. Hazard. Mater., 154 (2008) 337–346.
[38] L.S. Balistrieri, J.W. Murray, The surface chemistry of goethite (α-FeOOH) in major ion seawater, Am. J. Sci., 281 (1981) 788–806.
[39] S.S.M. Hassan, N.S. Awwad, H.A. Aboterika, Removal of synthetic reactive dyes from textile wastewater by Sorel's cement, J. Hazard. Mater., 162 (2009) 994–999.
[40] S. Hong, C. Wen, J. He, F. Gan, Y. Ho, Adsorption thermodynamics of Methylene Blue onto bentonite, J. Hazard. Mater., 167 (2009) 630–633.
[41] V.J.P. Poots, G. McKay, J.J. Healy, The removal of acid dye from effluent using natural adsorbents-I Peat, Water Res., 10 (1976) 1061–1066.